UNIVERSITY OF CALIFORNIA SAN DIEGO

Open-loop Printing of Liquid Metal for the Low-cost Rapid Fabrication of Soft Sensors

A thesis submitted in partial satisfaction of the
requirements for the degree Master of Science

in

Engineering Sciences (Mechanical Engineering)

by

Junda Chen

Committee in charge:

Professor Michael Tolley, Chair
Professor Shengqiang Cai
Professor Tania Morimoto
Professor Yong-Lae Park

2021

The thesis of Junda Chen is approved, and it is acceptable
in quality and form for publication on microfilm and electronically.

University of California San Diego

2021

DEDICATION

I would like to dedicate this work to my family, mentors for their support throughout the graduate program. I am lucky to be born in a family which encourage me to pursue higher education without financial worries. And I am grateful to my mentors who support me with my research project. I won't be able to finish this work without any of them.

EPIGRAPH

Your mind will answer most questions if you learn to relax and wait for the answer

- William S. Burroughs

TABLE OF CONTENTS

LIST OF FIGURES

LIST OF ABBREVIATIONS

LM: Liquid Metal

eGaIn: Eutectic Gallium-Indium

SOD: Stand-off Distance between extruder and substrate

ACKNOWLEDGEMENTS

I would like to acknowledge Professor Michael Tolley for his support as my main advisor, and for providing a relaxing lab environment. I was lucky to work under his supervision and had the chance to work on this work which I had never seen before.

I would like to acknowledge Professor Yong-Lae Park for his precious advice at the beginning of my research project, I would not be able to complete project on time without his help. This project exists because of his amazing work on the same topic.

I would like to acknowledge Dr. Benjamin Shih for his mentorship, patience and encouragement throughout the past 2 years. It is my honor to be mentored by such a wonderful person.

I would like to acknowledge members of the Bioinspired Robotics & Design Lab (BRDL) for their advice on my work. Their excellent works were encouragement that motivated me to keep working so that I deserved to be their labmates.

I would also like to acknowledge generous funding from the Office of Naval Research, grant numbers N00014-17-1-2062 and N00014-18-1-2277.

Chapter 1-3 is coauthored with Junda Chen, Benjamin Shih, Yong-Lae Park, Michael Tolley. The thesis author was the primary author of these chapters.

ABSTRACT OF THE THESIS

Open-loop Printing of Liquid Metal for the Low-cost Rapid Fabrication of Soft Sensors

by

Junda Chen

Master of Science in Engineering Sciences (Mechanical Engineering)

University of California San Diego, 2021

Professor Michael Tolley, Chair

Soft sensors using a highly conductive liquid metal eGaIn(eutectic gallium-indium) are widely researched due to the increasing need for flexible sensors such as temperature sensors, haptic sensors, multi-modal sensors and force sensors. Manufacturing methods for these soft sensors have been explored including printing, injection, lithography and spraying. Among these methods, direct writing of eGaIn is the fastest and simplest method. Other methods are mostly conventional mold-based fabrication while printing does not require

complicated pre-processing of elastomer. Although existing printing methods are able to pattern the liquid metal into various designs within micro scale, these methods either require high-precision feedback control over SOD, extrusion rate, low stage velocity or modification of liquid metal. As a result, the low tolerance in parameters of printing or extra modification of liquid metal make it difficult to replicate the work. Therefore, as a trade-off between printing quality and tolerance in precision, in this paper we present two open loop liquid metal printing methods with higher tolerance in precision using a low-cost open source system without the need to modify property of liquid metal. We discuss how parameters and setup of the printer will affect the printing quality. We also discuss how well the printing methods can resist variation in substrate height. As an example of applications of the proposed methods, we manufacture a strain sensor using the proposed method and demonstrate calibration result of the sensor. In general, these printing methods are alternative ways to manufacture liquid metal sensors when high accuracy is not desired.

Introduction

Soft sensors have recently been growing in popularity due to their higher stretchability and flexibility compared to rigid sensors. There are various types of soft sensors including capacitive sensors with dielectric layers of conductive polymers [1][2], capacitive and resistive sensors using PDMS with structured carbon black [3], sensors using optical stretchable fibers [4][5], sensors using carbon nanotubes [6][7] and 3d printed sensors consisting of layers of nonconductive and conductive photopolymers [8].

Among these soft sensors, liquid metal eGaIn (eutectic Gallium-Indium) sensors have been popular because of the high conductivity of eGaIn, which contributes to high enhancement in sensitivity and precision. Furthermore, the property that eGaIn is liquid at room temperature allows the liquid metal sensors to have higher stretchability, flexibility, and wearability compared to other soft sensors. Many researchers have recently reported various types of liquid metal sensors, including tactile sensors for both temperature and contact force sensing [9], soft skin with sensor array that can distinguish different types of pokes and rubs using machine learning [10], multi-axis force sensors that can decouple normal force from shear force [11], multi-modal sensors that can simultaneously sense strain deformation and pressure [12], and multi-modal gloves that can monitor motions of hand and provide haptic and thermal feedback based on activities in VR world [13].

Various methods for manufacturing liquid metal sensors have been explored including printing [14]-[17], injection [12], lithography [18], spraying [19]. However, methods such as injection, lithography, and spraying often require complex manufacturing processes, long manufacturing cycles and expensive equipment. For injection, manufacturers first assemble

two layers of elastomer made from two different molds into a sensor with empty embedded channels. Then, the manufacturers inserted one syringe into the entrance for injecting liquid metal, and the other syringe into the exit for pumping air out from the channels. The injection process is difficult and has high risk of leaking, thus resulting in higher labor cost and possible waste of material. For lithography, manufacturers made molds containing microchannels, then cool and heat the liquid metal in order to transfer the liquid metal onto the elastomer, thus resulting in a more complex manufacturing process and longer manufacturing cycle. For spraying, manufacturers made masks with desired patterns and sprayed the liquid metal to ensure the complete cover of liquid metal. The spraying of liquid metal on mask resulted in waste of liquid metal and required more manual input. Whereas with printing, there was no need to make molds and does not rely as much on manual input. As a result, the printing method makes it easy to manufacture sensors with different designs and have shorter manufacturing cycle.

There are generally three types of liquid metal printing methods: direct printing, printing with modified liquid metal, and contact printing. Various direct printing methods have been reported including printing of liquid metal patterns on flat, inclined, and curved elastomer [14], printing of free standing of liquid metal structures without the need of complex substrates [17], printing of liquid metal on metal electrodes for connecting eGaIn-based electronics to typical electronic devices [16]. Printing methods with modified liquid metal include electrowetting-assisted printing which applies voltage between liquid metal and substrate during extrusion [20], printing with laser-sintered liquid metal nanoparticles [21]-[24], printing with paste-like modified liquid metal [25]. For contact printing, printing on selected paper using

ball pen or brush pen with properly oxidized liquid metal ink have been reported. Although these works can print consistent liquid metal patterns, they have some unsolved problems respectively. Direct printing methods rely on highly precise feedback control of the print gantry. They should use SOD smaller than 0.3 mm, stage velocity smaller than 10 mm/s, and pressure smaller than 5 kPa to achieve successful printing. Thus, direct printing methods require sensors to maintain proper SOD during the printing. Printing with modified liquid metal require complex modification process. For contact printing using ball pen or brush pen, although they are faster and have lower requirement in SOD, they still need extra treatment for liquid metal and these methods only work on selected paper-like material, which is flexible but not stretchable and thus not suitable methods for making stretchable liquid metal soft sensors. Furthermore, for ball pen printing, it also requires a sensor to maintain proper SOD during printing.

In this paper, we test two open-loop approaches to the continuous printing of LM patterns on stretchable substrates which could print with larger range of parameters, higher tolerance in SOD, higher stage velocity without the need to modify the LM and we verify that printing performance (variance of trace width) is maintained despite variation in height of substrates.

Chapter 1: Methods and Materials

To test our proposed printing methods, we modified an open-source 3D printer cartesian stage (Prusa i3) with a custom syringe extrusion print head, controlled using control code (grbl) on a microcontroller Arduino (both open-source). A major challenge with printing liquid metal is the high variability of trace width due to periodic bulges that can occur along the trace for inappropriate print settings. To address this challenge, we tested two main approaches: 1) high-flowrate printing, which is a direct printing method relying on extruding stream of liquid metal; and 2) contact printing method with a set of bristles attached to the print head that act like a paint brush to generate a consistent trace.

1.1: Printing Parameters

For bristle method and high-flowrate method, we adjusted three parameters: the stage velocity(movement speed of printer head), flowrate (by controlling the torque of DC motor in order to maintain a constant pressure), and SOD(stand-off distance between substrate and needle tip). In this work, we only used two values of flowrate, 0.68 ml/s and 2.3 ml/s. Liquid metal is extruded as stream (**Fig 8**). Value of 2.3 ml/s was chosen because it was the smallest flowrate which could extrude stable stream of liquid metal. With flowrate of 0.68 ml/s, liquid metal is extruded as droplets (**Fig 7**). This flowrate was the possible smallest value for our printer. For bristle method, since we used bristle with length of 2 mm, the SOD was defined as 2 mm when the bristle barely touched the substrate during the printing. Because we were using a compliant syringe needle, the needle would deform whenever there was friction between the bristle and substrate. With this property, we were able to calibrate the SOD

without a distance sensor by doing the following steps. We first started with a height at which we could observe contact between the bristle and the substrate. Then, when we were moving the printer head horizontally, we kept lifting the printer head with step of 0.1 mm until the needle was not bent by the friction.

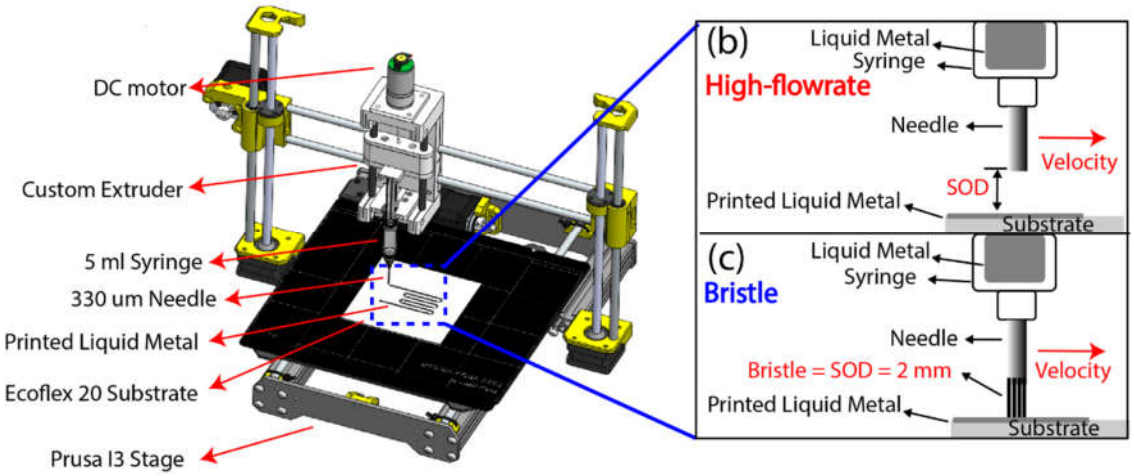

Figure 1: (a) Schematics of the printer. A needle with 330 μm (b) Schematic of high-flowrate method. (c) Schematic of bristle method. Bristle length we used was 2 mm, and thus the SOD is 2 mm when the bristle barely touches the substrate.

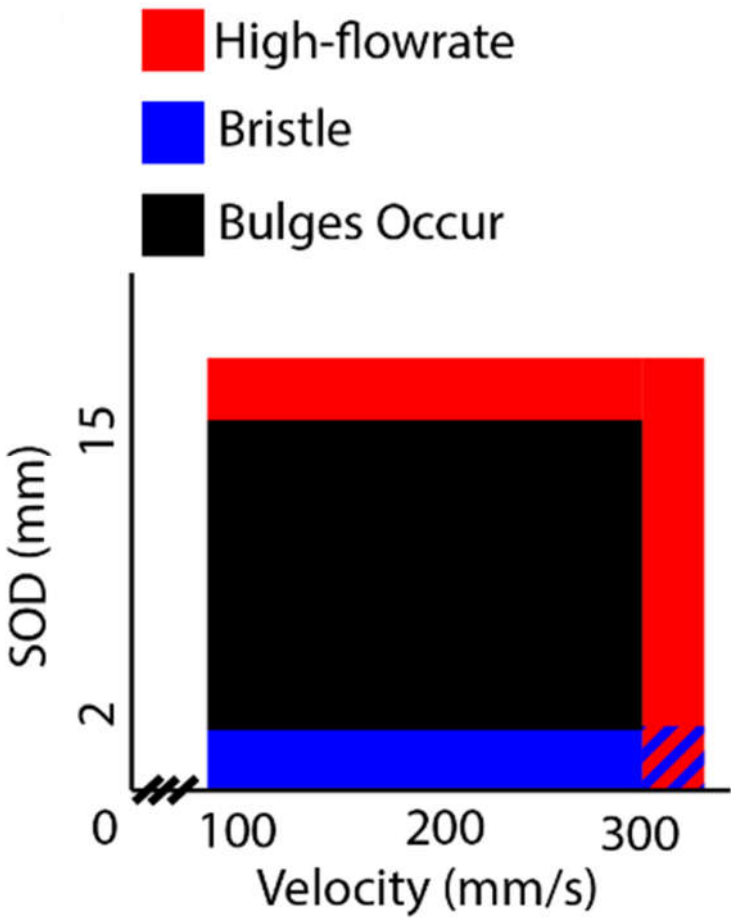

Figure 2: Plots demonstrating range of parameters for high-flowrate and bristle methods that print smooth traces without bulges. The red region represents that high-flowrate method can print traces without bulges when stage velocity is larger than 300 mm/s or SOD is larger than 15 mm using a constant flowrate of 2.3 ml/s. The blue region represents that the bristle method can print traces without bulges with SOD smaller than 2 mm, when the bristle is in touch with the printed liquid metal traces. It works with both flowrate of 0.68 ml/s and 2.3 ml/s. The black region represents parameters which print traces with bulges for both methods.

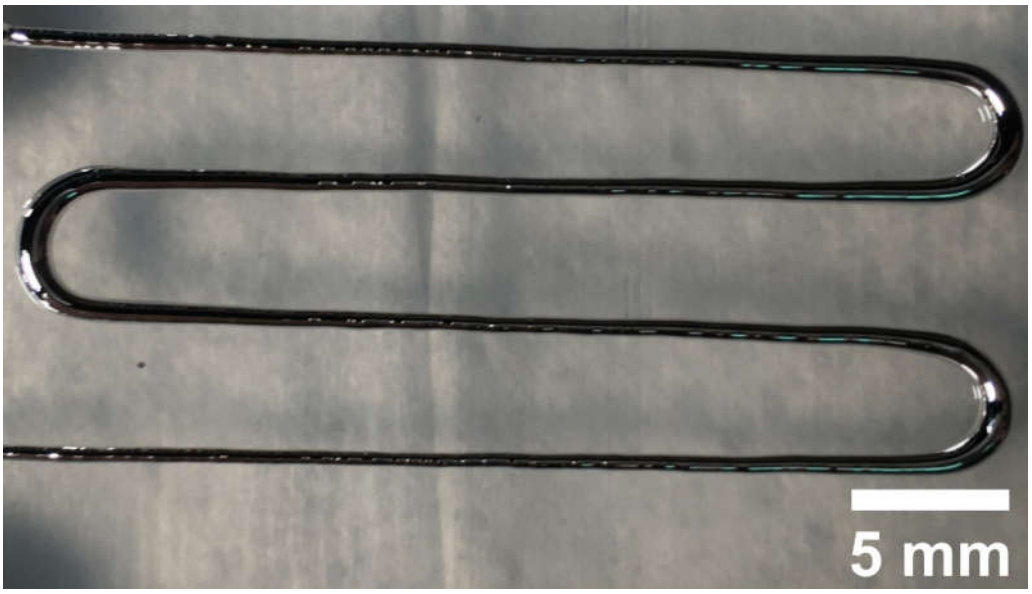

Figure 3: Top view of printed liquid metal strain pattern using bristle method.

Figure 4: Bird's-eye view of printed liquid metal strain pattern using bristle method.

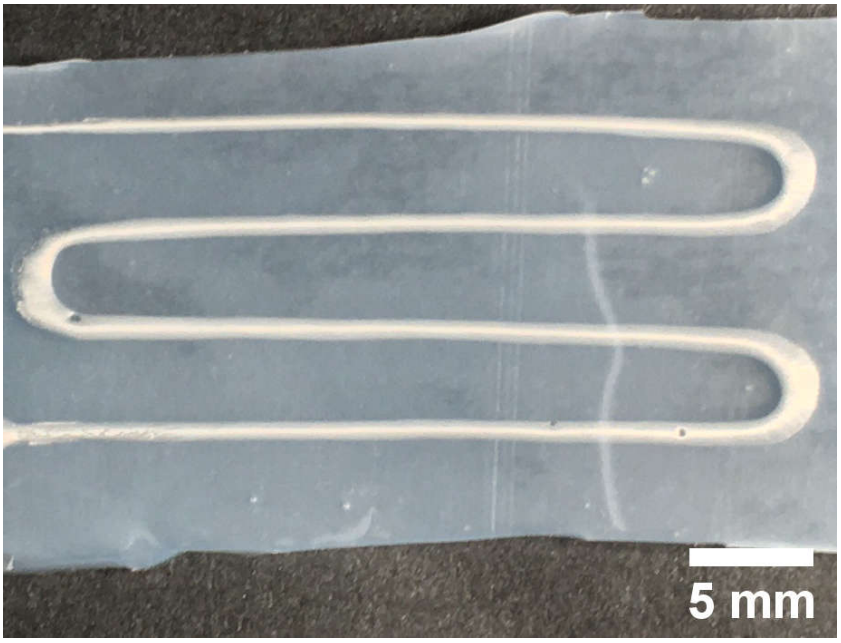

Figure 5: Top view of strain sensor made from the printed liquid metal pattern and silicone rubber (Ecoflex 20, Smooth-On).

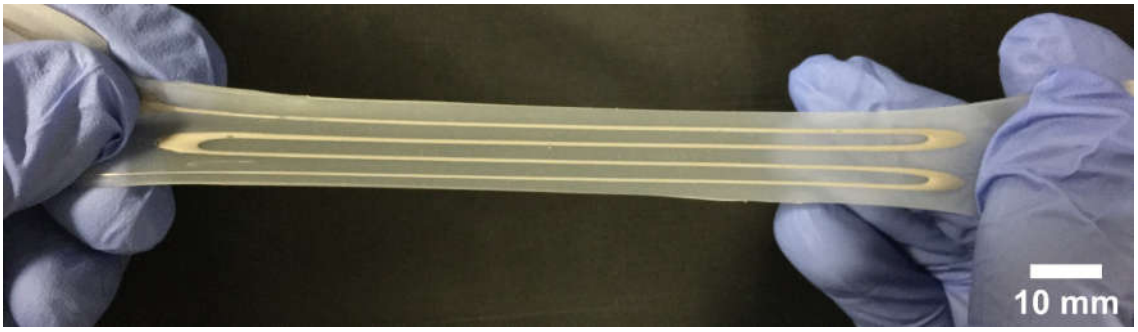

Figure 6: Sensor stretched to 300% strain.

1.2: Experimental Procedure

1.2.1: Effect of parameters on high-flowrate method

To test the effect of velocity and SOD on high-flowrate method, we conducted two set of experiments, in which we only changed either velocity or SOD. We printed eight 100 mm traces for each set of parameters and analyzed the average, variance of trace width and volume of bulges forming on the printed traces. In both set of experiment, we used a constant flowrate of 2.3 ml/s, which is a high flowrate such that the liquid metal is extruded as stream (**Fig 8**). If we use smaller flowrate, which extrudes liquid metal as droplet (**Fig 7**), the high-flowrate method will print discontinuous liquid metal traces as shown in **Fig 15**. In the first set of experiment, we fixed SOD at 2 mm, and increased velocity in the order of 100 mm/s, 200 mm/s, 300 mm/s. In the second set of experiment, we fixed velocity at 100 mm/s, and increased SOD in the order of 1 mm, 8 mm, 15 mm.

Figure 7: Liquid metal extruded as droplets using low flowrate 0.68 ml/s.

Figure 8: Liquid metal extruded as stream using high flowrate 2.3 ml/s.

1.2.2: Comparison between bristle and high-flowrate method

To compare the performance of high-flowrate and bristle methods, in this part we set the SOD as 2 mm for both high-flowrate and bristle methods. Since bristle method is capable of printing continuous liquid metal traces using both small and high flowrate, in this part we tested the bristle method using various velocity (100, 200, 300 mm/s) and flowrate (0.68 ml/s or 2.3 ml/s). We compared the performance of both methods to demonstrate the bristle method's capability to print with wider range of parameters and better printing quality. We printed eight 100 mm traces for each set of parameters and analyzed the average and variance of trace width.

Figure 9: Stranded wire bristle attached at the tip of the needle.

1.2.3: Effect of variation of substrate height

Since previous printing method should print with high precision in SOD(<0.3 mm), any variation in substrate height will significantly affect the printing result. However, variation in substrate height highly depends on its manufacturing process and the variation is unavoidable. Therefore, it would be necessary to test how well the new methods can resist the variation in height. This will also enable us to test whether these methods can work on non-planar surface without the need of adjusting SOD during printing. In this part, we used velocity of 300 mm/s and high flowrate of 2.3 ml/s for all the tests. We used both methods to print 8 traces with decreasing SOD (**Fig 10**) or increasing SOD (**Fig 11**) respectively. The printing started with SOD of 2 mm, and then changed by steps in the order of 0.8 mm, 0.6 mm, 0.4 mm, and 0.2 mm. The total change of SOD was ±2 mm.

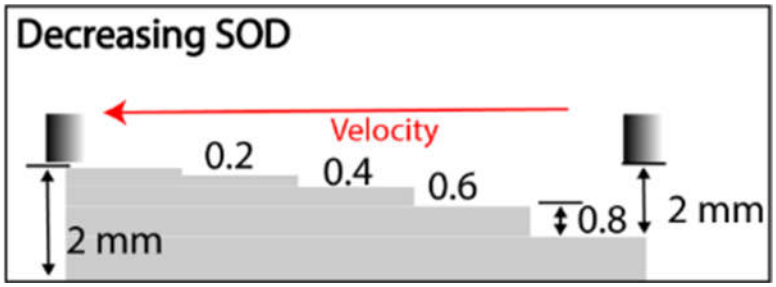

Figure 10: Schematics of printing with decreasing SOD. The SOD decreased from 2 mm to 0 mm.

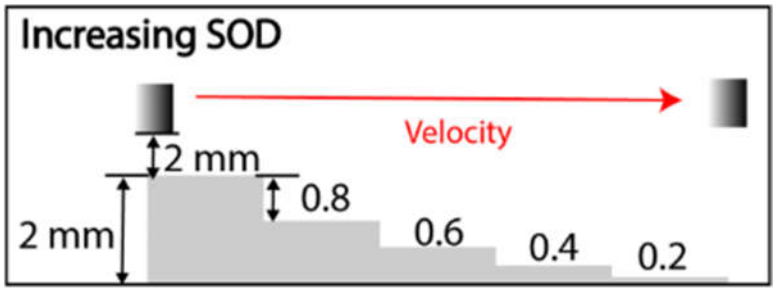

Figure 11: Schematics of printing with increasing SOD. The SOD increased from 2 mm to 4 mm.

Chapter 2: Results

2.1: Effect of parameters on high-flowrate method

The relationship between printing quality and stage velocity or SOD are plotted in **Fig 12** and **Fig 13**. When we printed with low SOD at 2 mm and high flowrate (**Fig 12**), bulges of liquid metal formed when the velocity was not high enough, leading to extra liquid metal printed on the traces. Increasing the stage velocity could efficiently decrease the occurrence of bulges of liquid metal (**Fig 14**), resulting in lower variance of trace width and less volume of bulges on traces. Using the 2 mm of SOD and high flowrate, the stage velocity should be increased to 300 mm/s in order to print traces without bulges. When we printed with low stage velocity at 100 mm/s and high flowrate (**Fig 13**), the volume of bulges decreased as we increased the SOD. Therefore, when we print with high-flowrate method, we could improve the printing quality by increasing the stage velocity or SOD. At stage velocity of 100 mm/s and high flowrate, the SOD should be increased to 15 mm such that the printed traces did not have bulges formed. If we use low flowrate, high-flowrate method can only print discontinuous traces as shown in **Fig 15** since we are not able to maintain a proper SOD smaller than 0.3 mm during the printing even if we use the correct flowrate and stage velocity suggested by previous works.

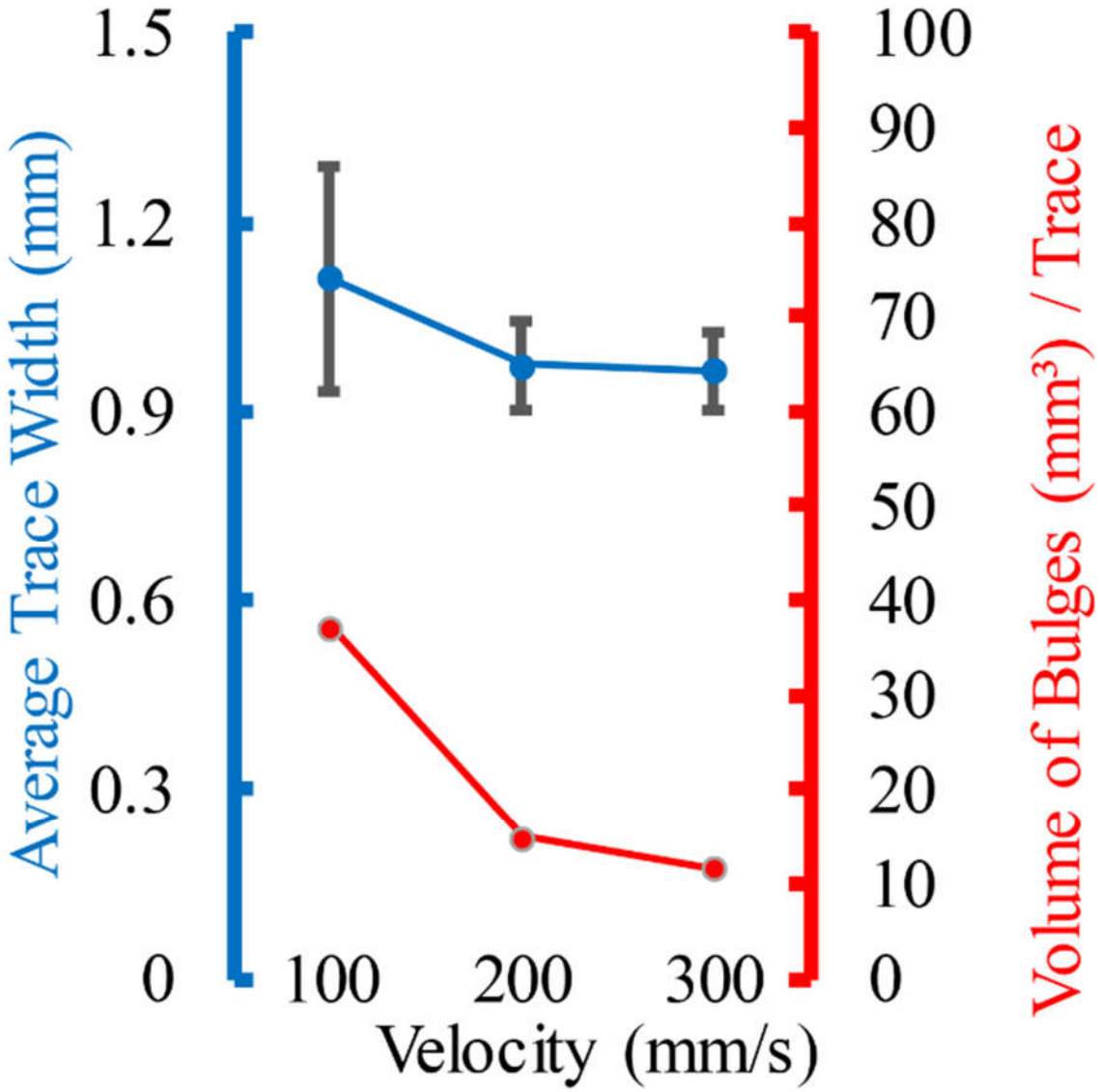

Figure 12: High-flowrate method's effect of velocity on trace width using high flowrate and 2 mm of SOD. The variance of trace width and volume of bulges on traces decrease as the stage velocity increases.

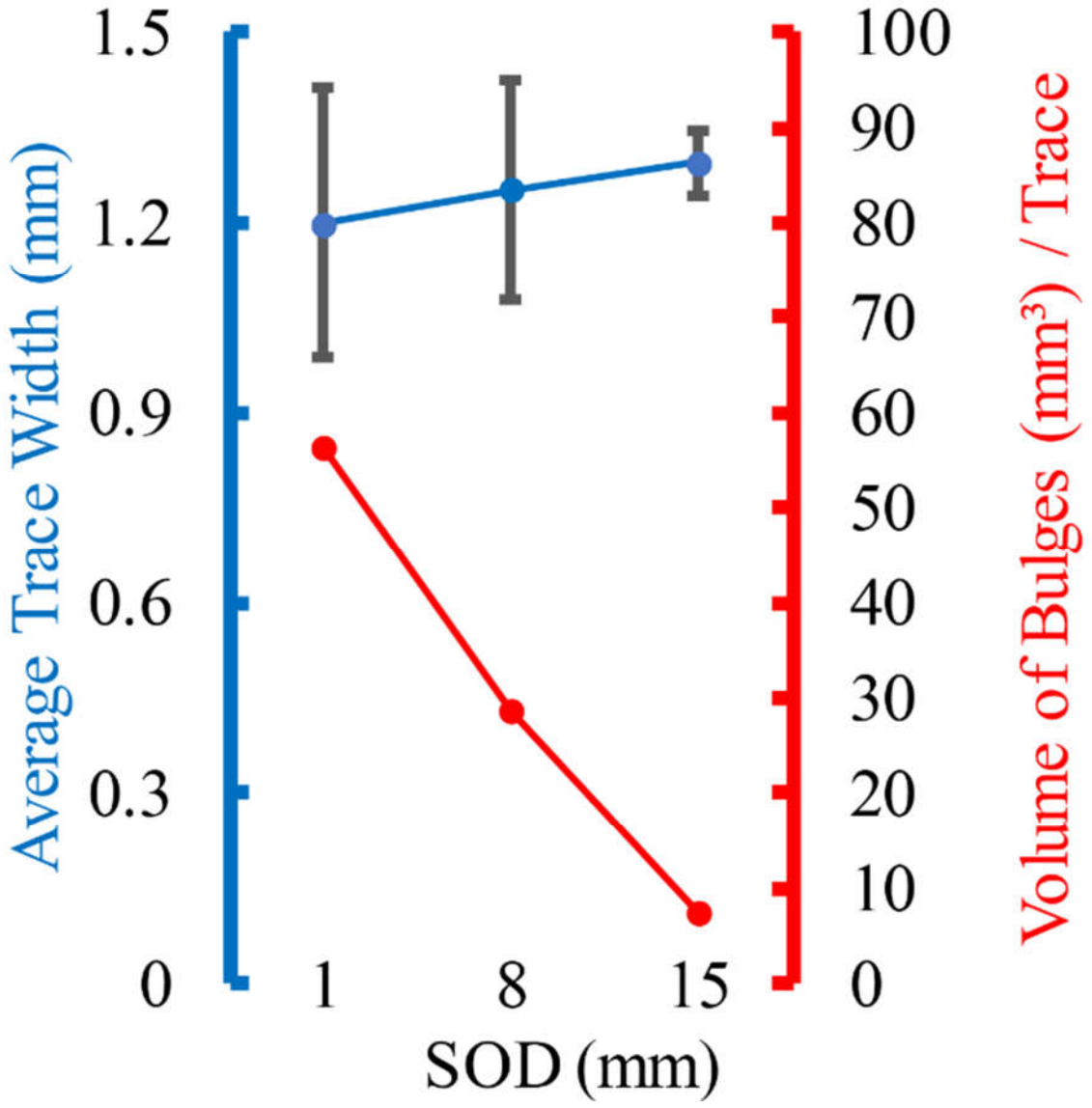

Figure 13: High-flowrate method's effect of SOD on trace width using high flowrate and 100 mm/s of velocity. The variance of trace width and volume of bulges on traces decrease as the SOD increases.

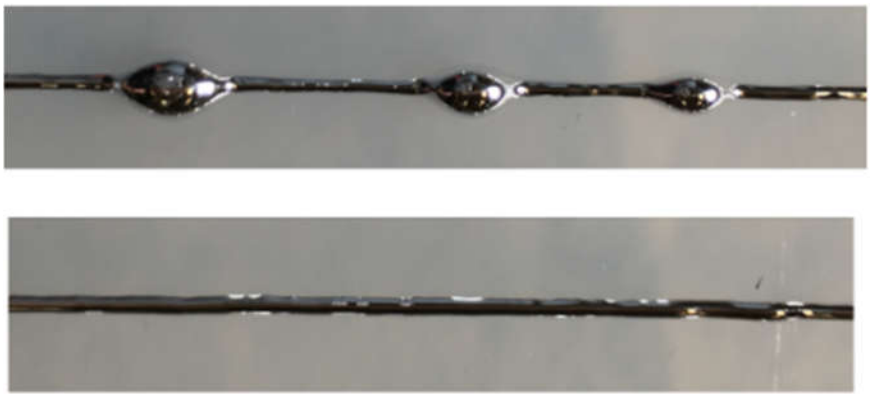

Figure 14: Top: trace with high variance using high-flowrate method. This occurs when extra liquid metal is printed. Bottom: trace with low variance using high-flowrate method when proper amount of liquid metal is printed.

Figure 15: Failed printing with high-flowrate method using SOD larger than 0.3 mm, velocity around 10 mm/s and low flowrate.

2.2: Comparison between bristle and high-flowrate method

As shown in **Fig 16**, when we used high flowrate, unlike high-flowrate method which printed traces with less bulges as the stage velocity increased, bristle method was able to print traces without bulges even at low stage velocity around 100 mm/s. But traces printed by bristle method generally had larger average trace width since the traces were flattened by the bristle. Meanwhile, although the high-flowrate method failed to print continuous traces using low flowrate, the bristle method was able to print continuous traces without bulges using low flowrate. At low flowrate, when the stage velocity was set to 300 mm/s, the volume of extruded liquid metal was not sufficient to print continuous traces thus we did not include this set of data in the plot. In general, the bristle method could print continuous traces without bulges using larger range of stage velocity and flowrate compared to the high-flowrate method. The bristle helps to smooth the traces and prevent bulges from forming during the printing. The bristle method also has better printing quality compared to high-flowrate method.

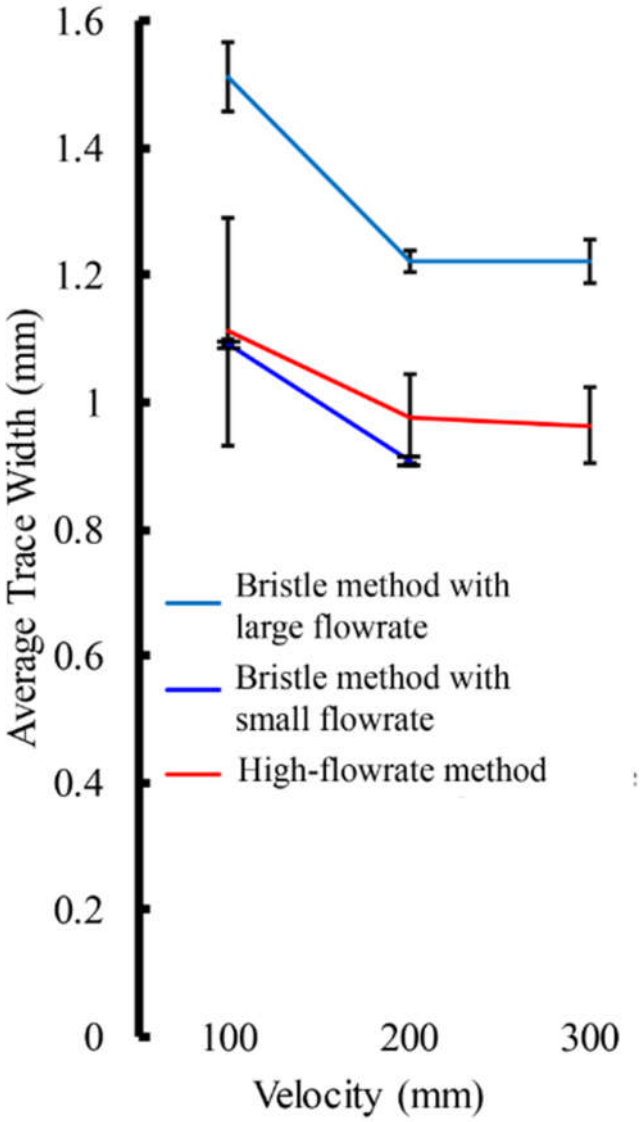

Figure 16: Comparison between high-flowrate and bristle method using varying velocity and flowrate. Compared to the high-flowrate method, the bristle method can print traces with consistent trace width using both low and high flowrate. It can also print traces using velocity at which high-flowrate method prints traces with bulges.

Figure 17: Trace with low variance printed by bristle method.

2.3: Effect of variation of substrate height

As shown in **Fig 18** and **Fig 19**, for both methods, the average and variance of trace width do not vary much when the SOD changed.

For printing with decreasing SOD (**Fig 18**), the bristle method had smaller and more stable variance of trace width than high-flowrate method. With the bristle touching the liquid metal traces, the printing performance did not diminish throughout the printing.

For printing with increasing SOD (**Fig 19**), the variance of trace width for bristle method was larger than high-flowrate method. As the bristle lost contact with the liquid metal traces, it worked similarly as the high-flowrate method, while the bristle was disturbing the extrusion and thus resulted in larger variance in trace width.

For high-flowrate method, the variation in SOD does not change the average or variance of the traces for both increasing and decreasing SOD. Thus demonstrating larger tolerance in SOD compared to traditional methods, which can only work with SOD smaller than 0.3 mm.

While for bristle method, when SOD is increasing, the bristle loses contact with the printed liquid metal. It fails to prevent forming of bulges and the variance of trace width increases resulted from disturbance of extrusion by the bristle. when SOD is decreasing, the bristle keeps contact with the printed liquid metal thus does not affect the print quality much.

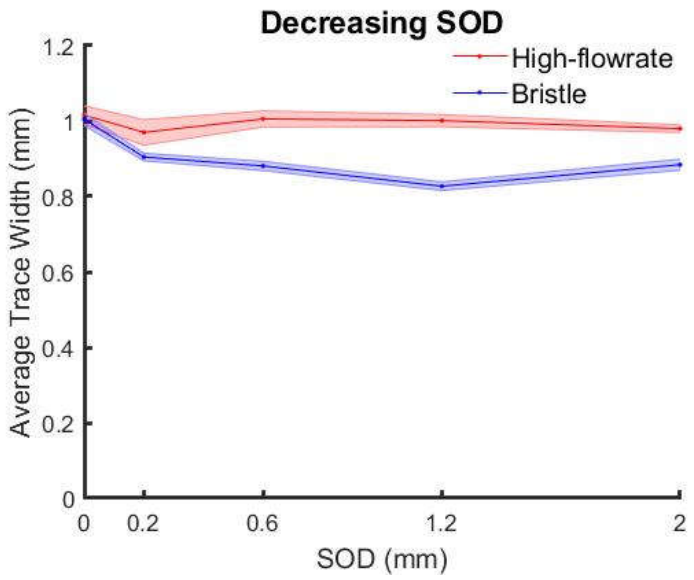

Figure 18: Effect of decreasing SOD on trace width and its variance for both methods.

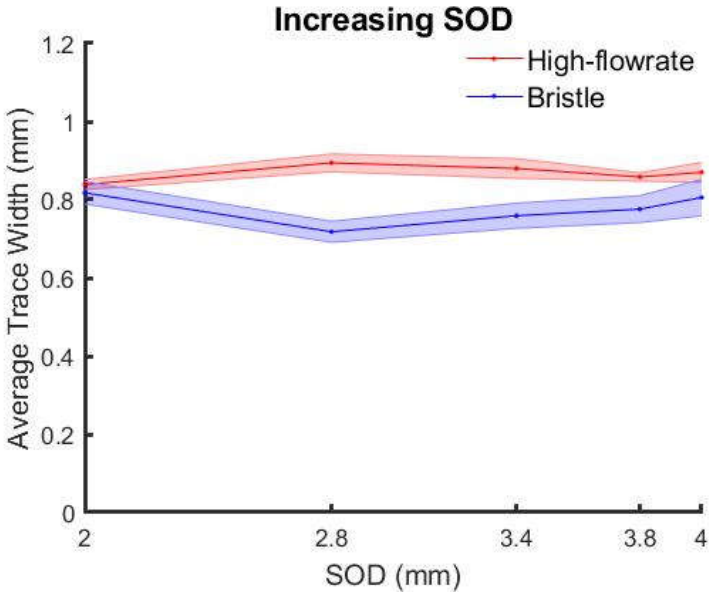

Figure 19: Effect of increasing SOD on trace width and its variance for both methods.

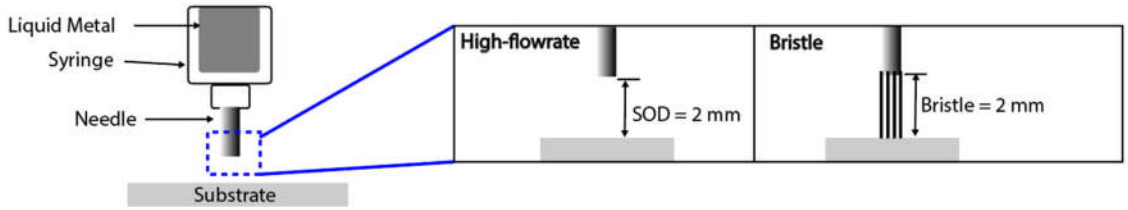

Figure 20: Schematics of high-flowrate and high-flowrate methods. For bristle method, we used bristle with length of 2 mm, and the SOD is 2 mm when the bristle barely touches the substrate at the beginning of the printing.

Chapter 3: Applications

In order to verify whether the proposed methods are suitable for manufacturing sensors, we then tested the proposed methods by printing strain patterns and calibrated a strain sensor made from the liquid metal strain pattern printed by bristle method.

3.1: Actual performance in printing commonly used strain patterns

After testing the performance of both printing methods, we would like to study their performance in printing complex patterns. In this work, we chose to print the commonly used strain patterns. We used velocity of 300 mm/s, constant high flowrate of 2.3 ml/s and SOD of 2 mm for both methods. We chose this set of parameters since it works for both methods.

When we used the high-flowrate method to print the strain pattern with length of 30 mm, gap width of 5 mm, bulges form consistently around the corners of the strain pattern. As we discussed above, the high-flowrate method should maintain a high stage velocity in order not to print extra liquid metal, which leads to bulges on traces. Due to the limitation in hardware of our printer, the acceleration of the printer was not large enough for the printer to maintain a high stage velocity when it was turning around corners (**Fig 21**). To eliminate the bulges, we increased the gap width of the strain pattern from 5 mm to 10 mm. The curvature of the strain pattern was large enough such that the stage velocity was high enough to prevent forming of bulges during the printing (**Fig 22**). The other solution to eliminate bulges is to use variable flowrate during the printing such that less liquid metal is printed around corners. [15]

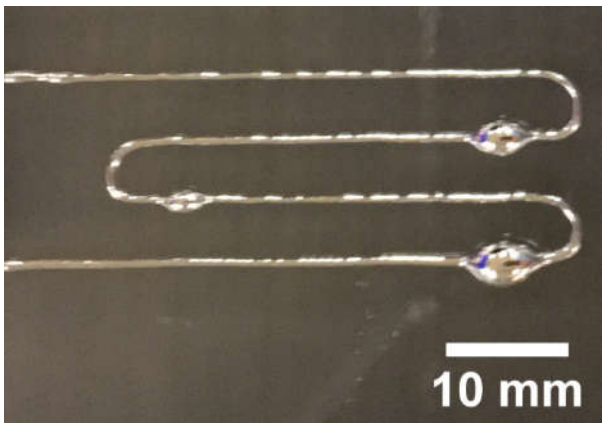

Figure 21: High-flowrate method printed bulges of liquid metal at corners of strain pattern with 5 mm gap.

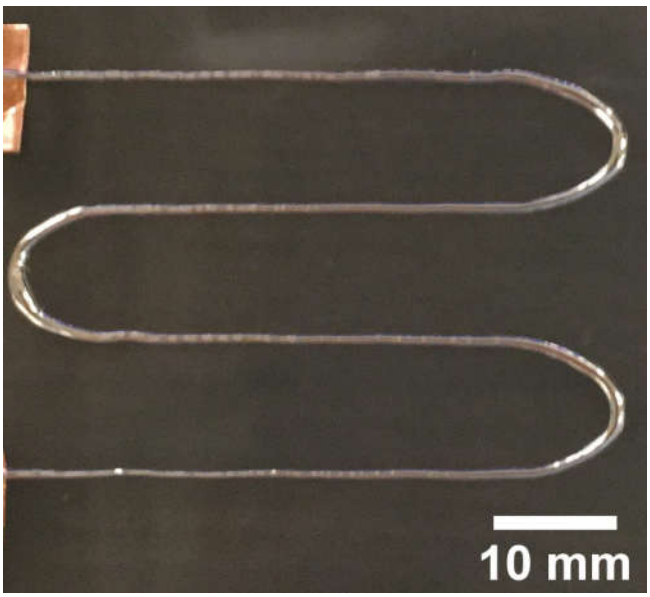

Figure 22: Bulges did not occur for high-flowrate method printing strain pattern with 10 mm gap.

When we used the bristle method to print the strain pattern with length of 30 mm, gap width of 5 mm, friction between the bristle and substrate led to the forming of bulges at corners of the strain pattern (**Fig 23**). As we mentioned, we were using a compliant needle and thus the needle and bristle were bent when the friction between the bristle and substrate was too large. Therefore, when the printer was turning around the corners, the needle tip stopped at the corners even when the extruder itself was moving (**Fig 25**). To solve this issue, we needed to make sure that the bristle barely touches the substrate to achieve a successful printing (**Fig 24**). Other possible solutions include using rigid needle or using proper materials for bristle to reduce friction.

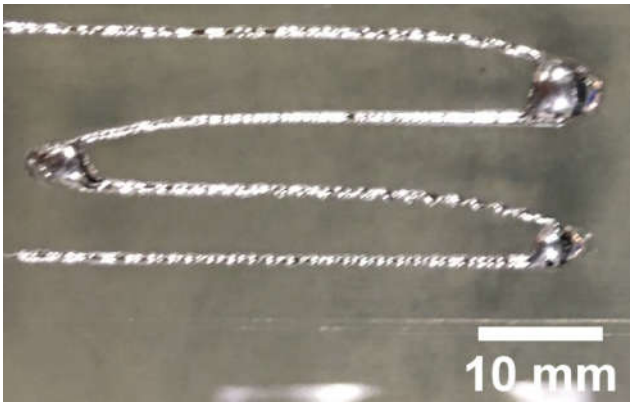

Figure 23: Needle was bent when the bristle touched the substrate, causing the needle tip to stop around corners of strain pattern.

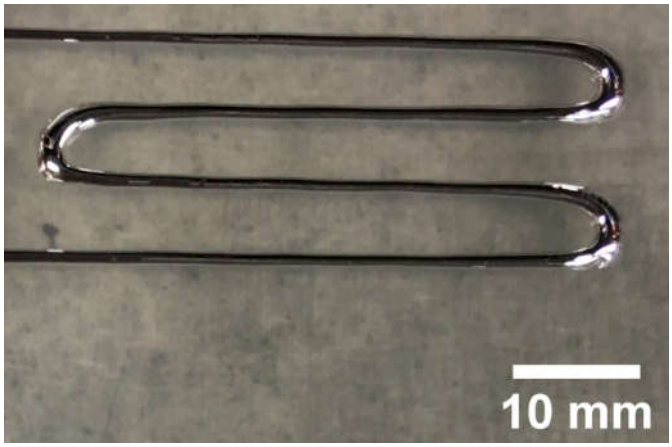

Figure 24: Bristle method printed strain pattern with 5 mm gap successfully with proper SOD.

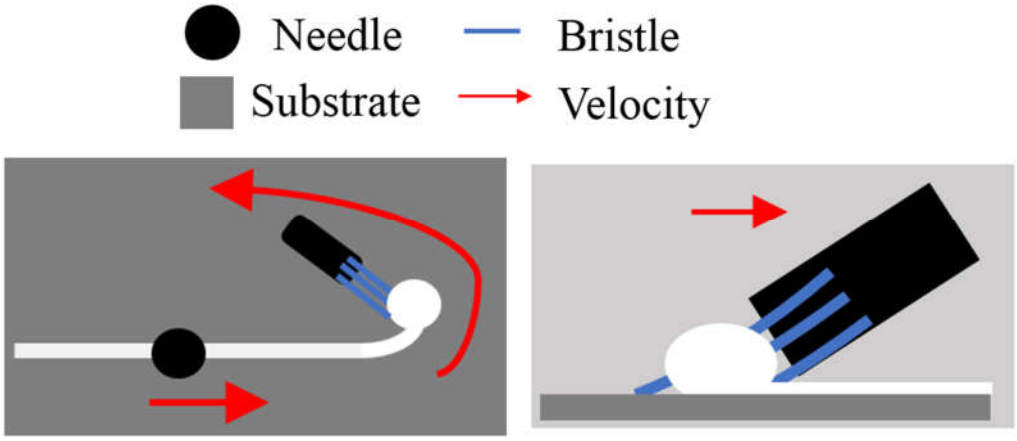

Figure 25: Bristle and needle bent when friction between bristle and substrate is too large, causing bulges to form at corners of strain pattern.

3.2: Calibration of strain sensors

To verify that the printing method could manufacture functional sensors with similar performance as those manufactured by traditional methods. We made a strain sensor out of the strain pattern printed by bristle method by encapsulating the printed pattern into layers of silicone rubber. Then we stretched the sensor up to 100\% strain using speed of 2 mm/s, 4 mm/s and 8 mm/s. According to the results, the change in resistance of the sensor is approximately linear to the strain and it slightly decreases as the stretching speed increases (**Fig 26**). These behaviors are similar to that of strain sensors manufactured by traditional injection method. [12]

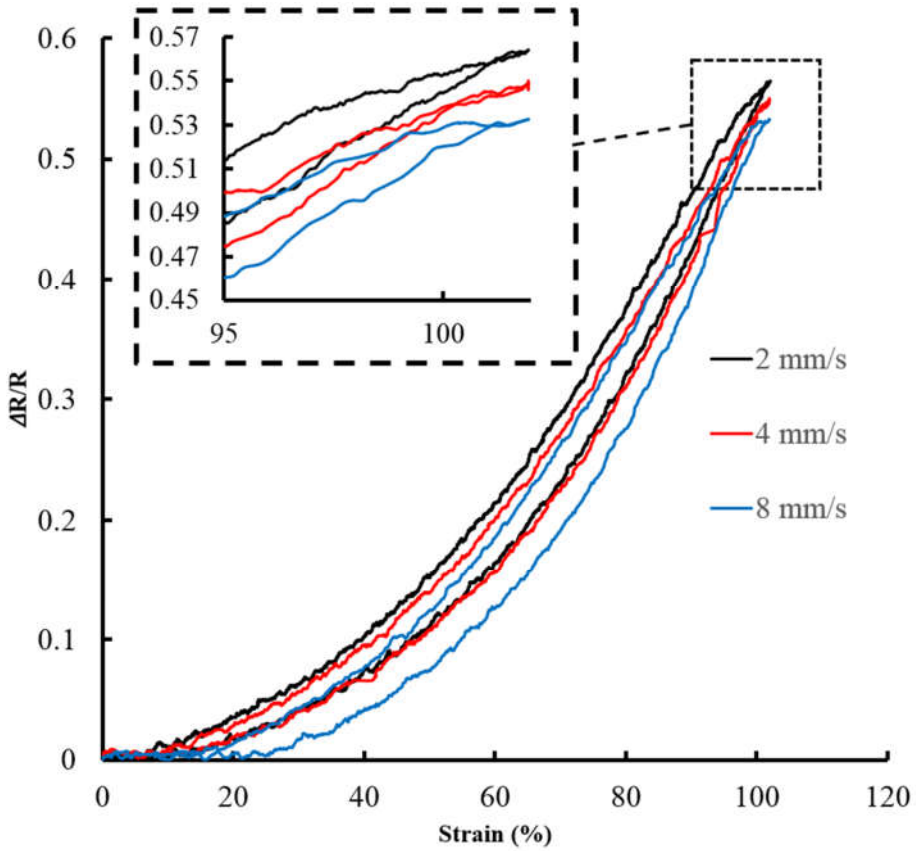

Figure 26: Calibration result of strain sensor with different stretching speed.

Chapter 4: Discussion

High-flowrate liquid metal printing method could print continuous and consistent liquid metal traces by using the combination of high flowrate, small SOD less than 2 mm and large stage velocity larger than 300 mm/s. When large stage velocity is not achievable, large SOD up to 15 mm should be used instead to prevent bulges. Compared to high-flowrate method, the attachment of bristle at the tip of the needle makes it possible to print with larger range of flowrate and stage velocity. As long as the bristle is in touch with the liquid metal traces, it is able to prevent bulges from forming even if extra liquid metal is printed. The high-flowrate method is able to maintain performance despite change of SOD up to 2 mm. While bristle method fails when the bristle loses contact with the liquid metal traces. Both methods demonstrate larger tolerance in SOD and wider range of parameters compared to previous printing methods. We also demonstrate calibration result of the strain sensor printed by proposed bristle method.

As a trade-off between roughness and accuracy, the proposed methods are not able to print micro scale patterns presented in previous works which use high-precision sensors and low stage velocity. Furthermore, minor variation in resistance of manufactured sensors exists due to open loop control of flowrate and SOD. The flowrate may vary depending on materials of syringe, oxidation levels of liquid metal and condition inside the syringe, which makes it hard to monitor the printed volume of liquid metal. These factors lead to unpredictable difference in manufacturing of sensors.

Since our printer could only print with constant flowrate, one possible future work to do is to test the performance of printing methods with variable flowrate so that strain patterns with

smaller curvature can be printed. In terms of the bristle method, future work to do is to find better designs of bristle including its material, length, and number of bristle. Furthermore, we should test more possible set of parameters for both methods and derive the relationship between the printed trace width and printing parameters.

In summary, the proposed methods are alternative way when high accuracy is not desired. They significantly accelerate printing of liquid metal on stretchable substrates and allows larger variation in manufacturing of substrates.

Chapter 1-3 is coauthored with Junda Chen, Benjamin Shih, Yong-Lae Park, Michael Tolley. The thesis author was the primary author of these chapters.

References

[1] H. Shi, M. Al-Rubaiai, C. M. Holbrook, J. Miao, T. Pinto, C. Wang, and X. Tan, “Screen-printed soft capacitive sensors for spatial map-ping of both positive and negative pressures,” Advanced Functional Materials, vol. 29, no. 23, p. 1809116, 2019.

[2] O. Atalay, A. Atalay, J. Gafford, and C. Walsh, “A highly sensitive capacitive-based soft pressure sensor based on a conductive fabricand a microporous dielectric layer,” Advanced materials technologies, vol. 3, no. 1, p. 1700237, 2018.

[3] R. P. Rocha, P. A. Lopes, A. T. de Almeida, M. Tavakoli, and C. Majidi, “Fabrication and characterization of bending and pressure sensors for a soft prosthetic hand,” Journal of Micromechanics and Microengineering, vol. 28, no. 3, p. 034001, 2018.

[4] J. Guo, X. Liu, N. Jiang, A. K. Yetisen, H. Yuk, C. Yang,A. Khademhosseini, X. Zhao, and S.-H. Yun, “Highly stretchable,strain sensing hydrogel optical fibers,” Advanced Materials, vol. 28,no. 46, pp. 10244–10249, 2016.

[5] P. A. Xu, A. K. Mishra, H. Bai, C. A. Aubin, L. Zullo, and R. F. Shepherd, “Optical lace for synthetic afferent neural networks,” Science robotics, vol. 4, no. 34, 2019.

[6] E. Roh, B.-U. Hwang, D. Kim, B.-Y. Kim, and N.-E. Lee, “Stretchable, transparent, ultrasensitive, and patchable strain sensor for human–machine interfaces comprising a nanohybrid of carbon nanotubes and conductive elastomers,” ACS nano, vol. 9, no. 6, pp. 6252–6261, 2015.

[7] S. Lee, A. Reuveny, J. Reeder, S. Lee, H. Jin, Q. Liu, T. Yokota,T. Sekitani, T. Isoyama, Y. Abe, et al., “A transparent bending-insensitive pressure sensor,” Nature nanotechnology, vol. 11, no. 5, pp. 472–478, 2016.

[8] B. Shih, J. Mayeda, Z. Huo, C. Christianson, and M. T. Tolley, “3dprinted resistive soft sensors,” in 2018 IEEE International Conference on Soft Robotics (RoboSoft), pp. 152–157, IEEE, 2018.

[9] Y. Wang, Y. Lu, D. Mei, and G. Qiang, “Development of wearable tactile sensor based on galinstan liquid metal for both temperature and contact force sensing,” in 2020 IEEE 16th International Conference on Automation Science and Engineering (CASE), pp. 442–448, IEEE,2020.

[10] B. Shih, E. Lathrop, I. Adibnazari, R. Martin, Y.-L. Park, and M. T.Tolley, “Classification of components of affective touch using rapidly-manufacturable soft sensor skins,” in 2020 3rd IEEE International Conference on Soft Robotics (RoboSoft), pp. 182–187, IEEE, 2020.

[11] T. Kim and Y.-L. Park, “A soft three-axis load cell using liquid-filled three-dimensional microchannels in a highly deformable elastomer,” IEEE Robotics and Automation Letters, vol. 3, no. 2, pp. 881–887,2018.

[12] Y.-L. Park, B.-R. Chen, and R. J. Wood, “Design and fabrication of soft artificial skin using embedded microchannels and liquid conductors,” IEEE Sensors journal, vol. 12, no. 8, pp. 2711–2718, 2012.

[13] J. Oh, S. Kim, S. Lee, S. Jeong, S. H. Ko, and J. Bae, “A liquid metal based multimodal sensor and haptic feedback device for thermal and tactile sensation generation in virtual reality,” Advanced Functional Materials, p. 2007772, 2020.

[14] G. Shin, B. Jeon, and Y.-L. Park, “Direct printing of sub-30 um liquid metal patterns on three-dimensional surfaces for stretchable electronics,” Journal of Micromechanics and Microengineering, vol. 30, no. 3, p. 034001, 2020.

[15] S. Kim, J. Oh, D. Jeong, W. Park, and J. Bae, “Consistent and reproducible direct ink writing of eutectic gallium–indium for high-quality soft sensors,” Soft robotics, vol. 5, no. 5, pp. 601–612, 2018.

[16] S. Kim, J. Oh, D. Jeong, and J. Bae, “Direct wiring of eutectic gallium–indium to a metal electrode for soft sensor systems,” ACS applied materials & interfaces, vol. 11, no. 22, pp. 20557–20565,2019.

[17] C. Ladd, J.-H. So, J. Muth, and M. D. Dickey, “3d printing of freestanding liquid metal microstructures,” Advanced Materials, vol. 25, no. 36, pp. 5081–5085, 2013.

[18] T. Kim, D.-m. Kim, B. J. Lee, and J. Lee, “Soft and deformable sensors based on liquid metals,” Sensors, vol. 19, no. 19, p. 4250, 2019.

[19] R. Guo, L. Sheng, H. Gong, and J. Liu, “Liquid metal spiral coil enabled soft electromagnetic actuator,” Science China Technological Sciences, vol. 61, no. 4, pp. 516–521, 2018.

[20] A. M. Watson, A. B. Cook, and C. E. Tabor, “Electrowetting-assisted selective printing of liquid metal,” Advanced Engineering Materials, vol. 21, no. 10, p. 1900397, 2019.

[21] E. L. White, J. C. Case, and R. K. Kramer, “Reconfigurable logic devices connected with laser-sintered liquid metal nanoparticles,” in 2017 IEEE SENSORS, pp. 1–3, IEEE, 2017.

[22] S. Liu, M. C. Yuen, and R. Kramer-Bottiglio, “Reconfigurable electronic devices enabled by laser-sintered liquid metal nanoparticles,” Flexible and Printed Electronics, vol. 4, no. 1, p. 015004, 2019.

[23] S. Liu, M. C. Yuen, E. L. White, J. W. Boley, B. Deng, G. J. Cheng, and R. Kramer-Bottiglio, “Laser sintering of liquid metal nanoparticles for scalable manufacturing of soft and flexible electronics,” ACS applied materials & interfaces, vol. 10, no. 33, pp. 28232–28241,2018.

[24] S. Liu, S. N. Reed, M. J. Higgins, M. S. Titus, and R. Kramer-Bottiglio, “Oxide rupture-induced conductivity in liquid metal nanoparticles by laser and thermal sintering,” Nanoscale, vol. 11, no. 38, pp. 17615–17629, 2019.

[25] U. Daalkhaijav, O. D. Yirmibesoglu, S. Walker, and Y. Meng uc ,“ Rheological modification of liquid metal for additive manufacturing of stretchable electronics,” Advanced Materials Technologies, vol. 3, no. 4, p. 1700351, 2018.